AIAA Atmospheric Flight Mechanics Conference and Exhibit
20 - 23 August 2007, Hilton Head, South Carolina

AIAA 2007-6633

Implications and Mitigation of Radio Frequency Blackout during Reentry of Reusable Launch Vehicles

Richard A. Hartunian,[1] Gordon E. Stewart[2], Thomas J. Curtiss[3],
Stephen D. Fergason[4], and Robert W. Seibold[5]
The Aerospace Corporation, El Segundo, CA 90245-4691

and

Pradipta Shome[6]
Federal Aviation Administration, Washington, DC 20591

Reentering hypersonic vehicles become surrounded by a layer of dissociated plasma, consisting of ions and free electrons, during high-velocity passage through the upper atmosphere. The ionized layer or sheath can reflect and attenuate propagating electromagnetic waves severely, causing radio communications to be degraded or temporarily disrupted. This interruption in signal transmission and reception, or radio frequency (RF) blackout, is of concern for determination of vehicle position and vehicle control, key issues affecting public safety, especially for future manned flights where continuous contact with ground control will be crucial. Causes of RF blackout from plasma generation around vehicles during hypersonic reentry were reviewed. Methodologies for mitigating communications blackouts, applicable to reusable launch vehicles (RLVs) for commercial space, were surveyed. Interactions of RF signals with a known ionized layer, including reflection, attenuation, refraction, high-power breakdown limits, and effects of the plasma on antenna characteristics, were explored. RF blackout mitigation strategies fall into two general classes: passive and active. Passive approaches necessitate design of vehicle configurations to minimize plasma effects on communications signals. Active approaches entail manipulation of the plasma conditions and electron density in localized regions surrounding communication antennas to facilitate RF transmission. Examples of passive approaches include: using vehicles with leading edges aerodynamically shaped to minimize plasma generation, designing for communication at higher frequencies, and designing for radiating higher power from the vehicle. Examples of active approaches include: injection of electrophilic quenchants or droplets that evaporatively cool the plasma and application of magnetic fields. The most promising approaches for mitigating the interruption of communications due to interactions of plasma electrons with RF signals are aerodynamic shaping, injection of electrophilic quenchants, use of magnetic windows, and use of high frequencies within the limits imposed by atmospheric attenuation.

Nomenclature

C_p = heat capacity
k_B = backward rate coefficient
k_F = forward rate coefficient

---

[1] Retired Vice President, Space Launch Operations, 8 Old Marsh Rd., Henderson, NV 89052, AIAA Fellow Retired.
[2] Senior Engineering Specialist, Antenna Systems Dept., 900 Meyer Lane, Redondo Beach, CA 90278-5216.
[3] Director, Propulsion Science Dept., 2350 E. El Segundo Blvd, MS M2-341.
[4] Present Address: Lockheed Martin Space Systems Company, P.O. Box 179, MS W3002, Denver, CO 80201.
[5] Senior Project Engineer, Space Launch Projects, 2350 E. El Segundo Blvd, MS M1-132, AIAA Member.
[6] Aerospace Engineer, Office of Commercial Space Transportation, AST-300, 800 Independence Avenue, S.W., #331.

N_e = electron density
R_N = nose radius
S = distance along surface of body from nosetip
T = temperature
U = flow velocity
U_∞ = free stream velocity
y = distance normal to body surface
Δ = shock standoff distance
ξ = S/R_N = ratio of downstream position to hemisphere radius

I. Introduction

BLACKOUT is caused when RF transmission waves used for communication, telemetry, or guidance are attenuated and/or reflected by electrons in the plasma sheaths surrounding vehicles during hypersonic reentry. These sheaths containing electrons result from extreme heating of the air by strong shock waves originating at leading edges of blunt vehicles, and from viscous dissipation of a layer of air on the surface of sharp leading-edge vehicles, e.g., those with nose radius ¼-in. or less.[1,2] In general, transmission is possible at RF frequencies greater than the characteristic "plasma frequency," a plasma parameter that scales with the square root of the electron density in plasma sheaths. Electron densities depend strongly on the vehicle shape, altitude, and velocity (and therefore temperature of the plasma sheath), and the angle of attack (AoA) of vehicle surfaces with respect to the direction of flight. During reentry, vehicles can generate high electron densities with plasma frequencies exceeding the RF transmission frequency, leading to communication blackouts. Communication is restored when plasma frequencies decrease, due mostly to deceleration to lower vehicle velocities and an increase in electron collision frequency with neutral particles due to the higher density of the plasma at lower altitudes.

II. Approach

This study addressed four goals: First, vehicle classes to be evaluated were defined. These included RLVs most likely to be used for space transportation in the future and other classes selected because of published flight data relevant to the reentry blackout problem. Secondly, ionized flow fields for each vehicle class were defined over a characteristic trajectory. In the absence of published flight data, the best state-of-the-art flow field codes were used to predict the ionized flow field. In each case, the altitudes of onset and subsequent recovery from blackout were highlighted. Thirdly, RF interactions with the ionized flow fields were reviewed, including comparisons with flight data where available. Finally, mitigation methodologies were surveyed and promising concepts recommended for more detailed assessment in actual application to full-scale RLVs.

III. Representative Vehicle Classes

Simple axisymmetric bodies are usually categorized, for the purposes of plasma sheath analysis, as blunt- or sharp-nosed, depending on the dominant source of plasma formation. Thus, a blunt-nosed body is one whose sheath properties are determined by air that has passed through a normal or nearly normal strong shock wave with potential to create large volume flows of plasma, and a sharp-nosed, slender body is one whose sheath properties are determined by viscous dissipation in the boundary layer, which on a sharp-nosed vehicle is supplied with air that has passed through a weak oblique shock. Another distinguishing characteristic between blunt- and sharp-nosed vehicles is that for the former, the thickness of the plasma sheath on the conical part of the vehicle fills the volume of flow between the edge of the boundary layer of the RV and the oblique shock wave, whereas the analogous volume on sharp, slender reentry vehicles is void of plasma.[1] Schematic representations of plasma flow fields around blunt- and sharp-tipped reentering vehicles are depicted in Figs. 1 and 2, respectively.

Five representative vehicle classes were reviewed. The first four were two types of conical ballistic RVs, with blunt tips and sharp tips, respectively, unpowered lifting glide vehicles, of which the Space Shuttle is a primary representative, and powered air-breathing lifting vehicles, such as the X-43. The fifth class was the K-1 2-stage orbital cargo vehicle, under development at Rocketplane Kistler, Inc. (RpK), which was included so that this highly blunted "slightly lifting" configuration could be analyzed.

Powered air-breathing lifting vehicles such as the X-43 demonstrators are designed to achieve altitudes in the vicinity of 100 kft and to cruise at near-zero AoAs at Mach numbers ranging from 7 to 10. Given those parameters, combined with the fact that the vehicle designs must produce minimum drag and, therefore, will likely incorporate sharp leading edges, the probability of blackout issues for this vehicle class appears remote.

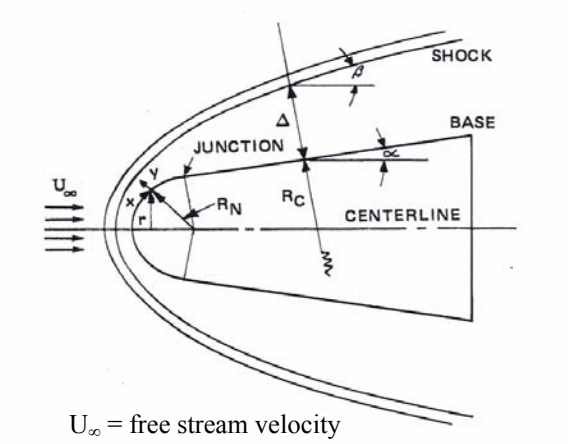

U_∞ = free stream velocity
Δ = shock standoff distance

Figure 1. Schematic flow field around a blunt-tipped RV.[3] *(Reprinted courtesy of NASA).*

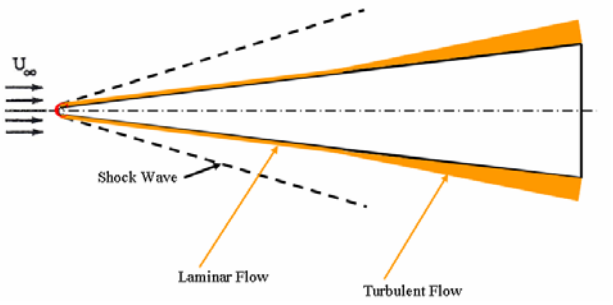

U_∞ = free stream velocity

Figure 2. Schematic flow field around a sharp-tipped RV.

Two specific types of ballistic vehicles are illustrated in Figs. 3 and 4, respectively. In Fig. 3, blunt conical ballistic RVs are represented by the NASA Radio Attenuation Measurements (RAM) flight experiments from the 1960s and 1970s, which addressed the blackout problem in a comprehensive manner for blunted vehicle configurations.[4] The highly blunted RpK K-1 vehicle is shown in Fig. 4. Unpowered lifting glide vehicles are represented in Fig. 5 by the Space Shuttle Orbiter, and powered air-breathing hypersonic cruise vehicles by the X-43A. A schematic representation of a sharp-tipped vehicle was depicted in Fig. 2.

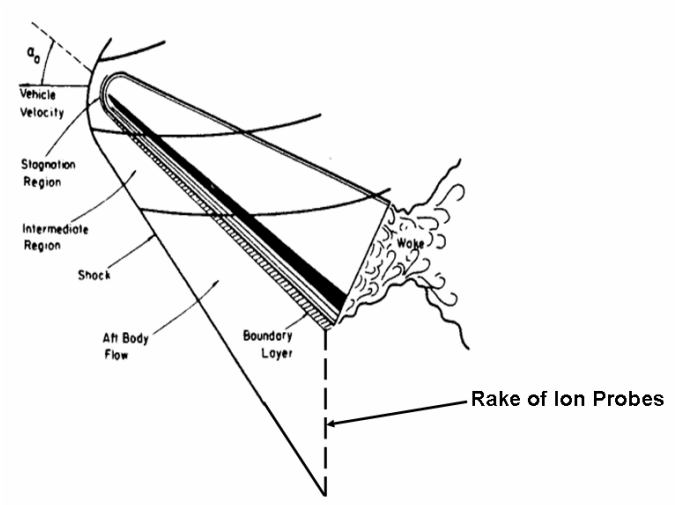

Figure 3. Schematic of RAM C vehicles and reentry flow characteristics[4]

Figure 4. Artist's conception of RpK K-1 vehicle. *(Reprinted with permission of Rocketplane Kistler, Inc.)*

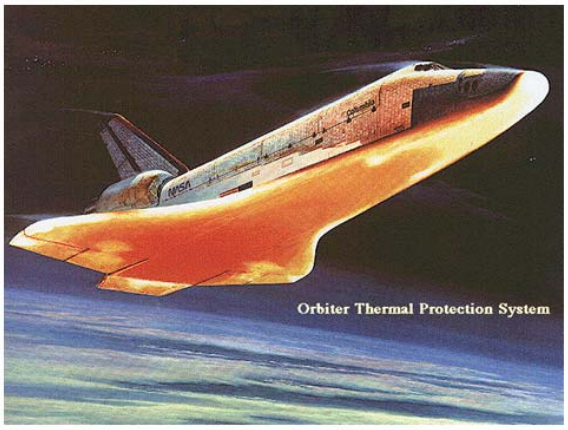

Drawing of Space Shuttle Orbiter During Reentry Conditions

X-43A Air-breathing Hypersonic Vehicle During Ground Testing

Figure 5. Unpowered glide and powered cruise vehicles. *(Reprinted courtesy of NASA).*

IV. Sources of Electrons on Plasma Sheaths

Equation (1) quantifies conservation of energy from velocity to temperature for the direction normal (90º) to vehicle's velocity vector. As the velocity decreases, heat capacity times temperature increases as indicated.

$$(C_pT)_{atm} + U^2/2 = \text{constant for normal flow across a 1-D shock wave} \quad (1)$$

where: C_p = heat capacity, T = temperature, U = flow velocity

As the temperature increases, a two-step process occurs. The first step is excitement of molecule translation, rotation, and vibration modes. The second step is molecular dissociation and ionization. These processes take thermal energy from the flow. The resulting endothermic reactions reduce the static temperature.

High reentry temperatures dissociate the oxygen and nitrogen molecules of the air, which triggers complex chemical reactions, recombining these molecules and producing ionization. All of these reactions need to be accounted for; twenty-six examples and concomitant forward and backward rate coefficients are listed in Table 1.[3] In the exothermic reactions, molecules collide with sufficient energy to overcome the activation energy barrier and form an activated complex at a lower energy level. The released electrons form the plasma sheath, inhibiting communications. At lower altitudes, the forward and reverse rates become equal, producing chemical equilibrium. At high altitudes, non-equilibrium chemistry prevails, complicating the analysis.

A. Plasma Flow Fields: Blunt, Slender Reentry Bodies

The NASA RAM Program (Fig. 3) addressed the blackout problem in a comprehensive manner. Nosetips with various degrees of bluntness on an aft body with a 9 degree half-angle were instrumented heavily and reentered at velocities of 18 kft/s in RAM Series A and B and 25 kft/s in Series C. For blunt vehicles such as these, the electrons form primarily in the nose region. As they flow downstream, they fill the area between the vehicle surface and the shock wave.

In the NASA RAM-C flight series, an electrostatic rake (Fig. 3) was used to measure ion densities in the shock layer, from which electron densities were deduced. The rake employed a blade-like design with a very sharp leading edge of 0.01-in. radius and held small metallic ion collectors.[5,6] The rake was mounted on the rear end of the conical heatshield and survived heating down to 180 kft altitude, at which point it was retracted to preclude melting of components.

The trajectory for the RAM C-II vehicles, i.e., velocity as a function of altitude, is shown in Fig. 6.[7] The RAM-C vehicles had a 6-inch nose radius and were 49 inches long. Microwave reflectometers measured electron number densities at four axial locations. Each reflectometer measured four frequencies, thus recording a distribution of electron densities from the wall out to the edge of the plasma layer. The objective was to provide accurate data for comparisons with the best available predictive codes. As seen in this figure, blackout of this blunt-nose

configuration occurred over a wide range of transmission frequencies. As expected, higher frequencies were associated with later onset of blackout.

Table 1. Chemical reactions and rate coefficients used in nonequilibrium calculations.[3]
(Reprinted courtesy of NASA).

NO.	REACTION	FORWARD RATE COEFF, k_F	BACKWARD RATE COEFF, k_B	THIRD BODY, M
	FORWARD DIRECTION	cm^3/mole sec	cm^3/mole sec OR cm^6/mole^2 sec	——
1	$O_2 + M \rightarrow 2O + M$	$3.6 \times 10^{18}\ T^{-1.0}\ \exp(-5.95 \times 10^4/T)$	$3.0 \times 10^{15}\ T^{-0.5}$	N, NO
2	$N_2 + M \rightarrow 2N + M$	$1.9 \times 10^{17}\ T^{-0.5}\ \exp(-1.13 \times 10^5/T)$	$1.1 \times 10^{16}\ T^{-0.5}$	O, NO, O_2
3	$NO + M \rightarrow N + O + M$	$3.9 \times 10^{20}\ T^{-1.5}\ \exp(-7.55 \times 10^4/T)$	$1.0 \times 10^{20}\ T^{-1.5}$	O_2, N_2
4	$O + NO \rightarrow N + O_2$	$3.2 \times 10^{9}\ T^{1}\ \exp(-1.97 \times 10^4/T)$	$1.3 \times 10^{10}\ T^{1.0}\ \exp(-3.58 \times 10^3/T)$	
5	$O + N_2 \rightarrow N + NO$	$7.0 \times 10^{13}\ \exp(-3.8 \times 10^4/T)$	1.56×10^{13}	
6	$N + N_2 \rightarrow N + N + N$	$4.085 \times 10^{22}\ T^{-1.5}\ \exp(-1.13 \times 10^5/T)$	$2.27 \times 10^{21}\ T^{-1.5}$	
7	$O + N \rightarrow NO^+ + e^-$	$(1.4 \pm 0.4) \times 10^{6}\ T^{1.5}\ \exp(-3.19 \times 10^4/T)$	$(6.7 \pm 2.3) \times 10^{21}\ T^{-1.5}$	
8	$O + e^- \rightarrow O^+ + e^- + e^-$	$(3.6 \pm 1.2) \times 10^{31}\ T^{-2.91}\ \exp(-1.58 \times 10^5/T)$	$(2.2 \pm 0.7) \times 10^{40}\ T^{-4.5}$	
9	$N + e^- \rightarrow N^+ + e^- + e^-$	$(1.1 \pm 0.4) \times 10^{32}\ T^{-3.14}\ \exp(-1.69 \times 10^5/T)$	$(2.2 \pm 0.7) \times 10^{40}\ T^{-4.5}$	
10	$O + O \rightarrow O_2^+ + e^-$	$(1.6 \pm 0.4) \times 10^{17}\ T^{-0.98}\ \exp(-8.08 \times 10^4/T)$	$(8.0 \pm 2.0) \times 10^{21}\ T^{-1.5}$	
11	$O + O_2^+ \rightarrow O_2 + O^+$	$2.92 \times 10^{18}\ T^{-1.11}\ \exp(-2.8 \times 10^4/T)$	$7.8 \times 10^{11}\ T^{0.5}$	
12	$N_2 + N^+ \rightarrow N + N_2^+$	$2.02 \times 10^{11}\ T^{0.81}\ \exp(-1.3 \times 10^4/T)$	$7.8 \times 10^{11}\ T^{0.5}$	
13	$N + N \rightarrow N_2^+ + e^-$	$(1.4 \pm 0.3) \times 10^{13} \exp(-6.78 \times 10^4/T)$	$(1.5 \pm 0.5) \times 10^{22}\ T^{-1.5}$	
14	$O_2 + N_2 \rightarrow NO + NO^+ + e^-$	$1.38 \times 10^{20}\ T^{-1.84}\ \exp(-1.41 \times 10^5/T)$	$1.0 \times 10^{24}\ T^{-2.5}$	
15	$NO + N_2 \rightarrow NO^+ + e^- + N_2$	$2.2 \times 10^{15}\ T^{-0.35}\ \exp(-1.08 \times 10^5/T)$	$2.2 \times 10^{26}\ T^{-2.5}$	
16	$O + NO^+ \rightarrow NO + O^+$	$3.63 \times 10^{15}\ T^{-0.6}\ \exp(-5.08 \times 10^4/T)$	1.5×10^{13}	
17	$N_2 + O^+ \rightarrow O + N_2^+$	$3.4 \times 10^{19}\ T^{-2.0}\ \exp(-2.3 \times 10^4/T)$	$2.48 \times 10^{19}\ T^{-2.2}$	
18	$N + NO^+ \rightarrow NO + N^+$	$1.0 \times 10^{19}\ T^{-0.93}\ \exp(-6.1 \times 10^4/T)$	4.8×10^{14}	
19	$O_2 + NO^+ \rightarrow NO + O_2^+$	$1.8 \times 10^{15}\ T^{0.17}\ \exp(-3.3 \times 10^4/T)$	$1.8 \times 10^{13}\ T^{0.5}$	
20	$O + NO^+ \rightarrow O_2 + N^+$	$1.34 \times 10^{13}\ T^{0.31}\ \exp(-7.727 \times 10^4/T)$	1.0×10^{14}	
21	$NO + O_2 \rightarrow NO^+ + e^- + O_2$	$8.8 \times 10^{15}\ T^{-0.35}\ \exp(-1.08 \times 10^5/T)$	$8.8 \times 10^{26}\ T^{-2.5}$	
22	$O_2 + O \rightarrow 2O + O$	$9.0 \times 10^{19}\ T^{-1.0}\ \exp(-5.95 \times 10^4/T)$	$7.5 \times 10^{16}\ T^{-0.5}$	
23	$O_2 + O_2 \rightarrow 2O + O_2$	$3.24 \times 10^{19}\ T^{-1.0}\ \exp(-5.95 \times 10^4/T)$	$2.7 \times 10^{16}\ T^{-0.5}$	
24	$O_2 + N_2 \rightarrow 2O + N_2$	$7.2 \times 10^{18}\ T^{-1.0}\ \exp(-5.95 \times 10^4/T)$	$6.0 \times 10^{15}\ T^{-0.5}$	
25	$N_2 + N_2 \rightarrow 2N + N_2$	$4.7 \times 10^{17}\ T^{-0.5}\ \exp(-1.13 \times 10^5/T)$	$2.72 \times 10^{16}\ T^{-0.5}$	
26	$NO + M \rightarrow N + O + M$	$7.8 \times 10^{20}\ T^{-1.5}\ \exp(-7.55 \times 10^4/T)$	$2.0 \times 10^{20}\ T^{-1.5}$	O, N, NO

B. Plasma Flow Fields: Sharp, Slender Reentry Bodies

The sharp-tipped configuration discussed here consisted of an axisymmetric cone body with a small half-angle and small nose radius. The flow field for this configuration consists of an oblique shock wave that forms along the length of the body and a thin boundary layer. Figure 2 depicts a turbulent boundary layer along the aft portion of the vehicle. In this case, the flow of molecules through the normal shock wave at the small nose generates electrons, but not enough to ionize a large portion of the flow. Instead, the boundary layer on the surface provides energy to increase the air temperature by viscous dissipation and thereby cause ionization.

Steiger et al. at The Aerospace Corporation reported that high-altitude telemetry blackout was experienced on a sharp-tipped, slender RV (Fig. 7)[2]. The vehicle was a sphere-cone with a ¼-inch nose radius, an 8° cone half-angle, and an X-band circumferential ring antenna at about the 5-in. station. Telemetry measurements indicated plasma attenuation beginning at approximately 190 kft and increasing to blackout conditions at approximately 145 kft. An analysis indicated that the main contributor to the signal degradation was plasma attenuation with pattern distortion, resulting from a small look angle. Further analysis indicated that a substantial reduction in plasma attenuation can be achieved either by sharpening the nose radius or by moving the antenna to a more aft location.

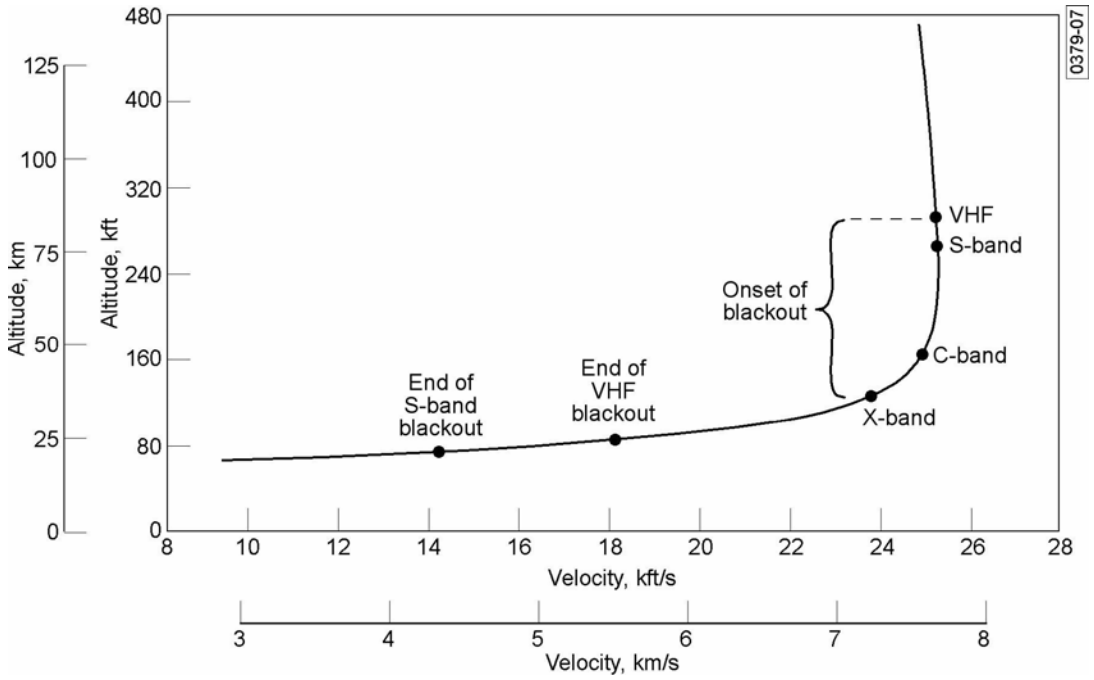

Figure 6. RAM C-II reentry trajectory showing onset and end of RF signal blackout. X-band and C-band reacquisition were delayed because of tracking difficulties.[7] (Reprinted courtesy of NASA).

C. Plasma Flow Fields: Unpowered Lifting Glide Vehicle

The Space Shuttle Orbiter is a well-known example of an unpowered lifting glide vehicle. There are no reported direct experimental measurements of the ionized flow field on a reentering Orbiter, for the obvious reason of not wishing to jeopardize safety by introducing instrumentation on the heat shield.

However, Dunn and Kang analyzed the ionized flow field in April 1973, about 8 years before the first Shuttle flight. They modeled the Orbiter as a 20° cone with a 4-ft. radius blunt nose reentering at 20° AoA. Despite the fact that the nose radius on the actual as-built Shuttle is smaller and the entry AoA is actually 40°, they concluded that blackout duration would be 15 minutes, close to the actual 16 minutes experienced.

Dunn and Kang's results are shown in Fig. 8. The abscissa on each plot is the distance across the plasma from the body to the shock at various locations along the body (S), divided by the nose radius.

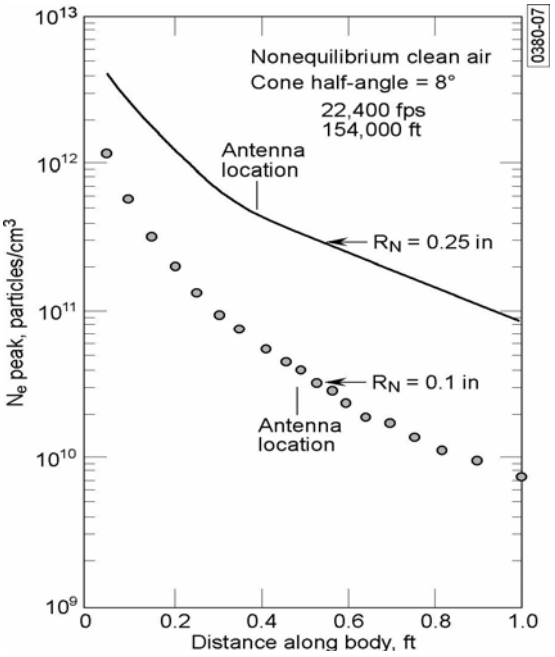

Figure 7. Clean air peak electron density decay.[2]

The left plot shows those electron density profiles at an altitude of 280 kft. The critical plasma density for S-band RF is 6.5 x 10^{10} electrons/cm^3. Similar values were seen further aft on the vehicle, and as the vehicle descends another 15 kft to 265 kft, the entire vehicle will be covered with critical plasma. When the antennas are covered with critical plasma, the RF will be totally reflected (blacked out) at high altitudes. The Shuttle flights eight years later experienced blackout onset at 265 kft.

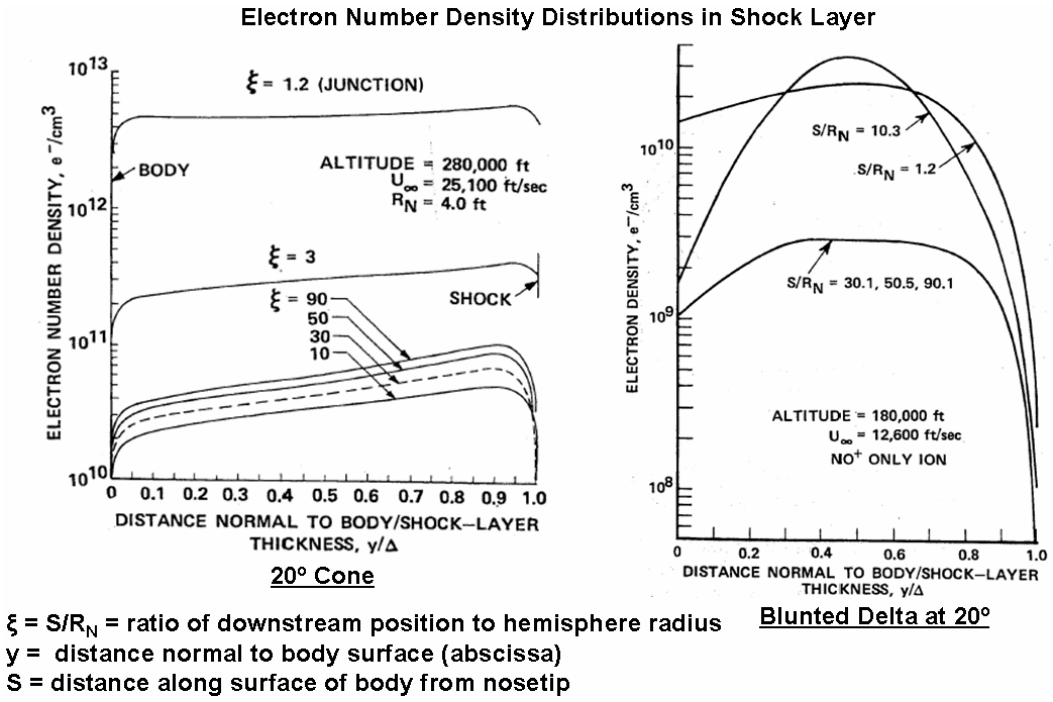

Figure 8. Plasma flow profiles for Shuttle configuration.[3] *(Reprinted courtesy of NASA).*

The right plot in Fig. 8 depicts the plasma shape at various locations along the body length for a delta-shaped wedge model of the Shuttle at an altitude of 180 kft. The peak electron density is seen to be below the critical plasma density, indicating recovery from blackout, which is 15 kft higher than where the Shuttle emerges from blackout.

From these results, Dunn and Kang concluded that the duration of blackout would be approximately 15 minutes.

D. Plasma Flow Fields: Fully Reusable Two-Stage Vehicle

Rocketplane Kistler (RpK) has been developing a two-stage launch vehicle, the K-1 (Fig. 9), designed to be fully recoverable. The first stage would fly to an altitude of 142 kft, separate from the second stage with its engines off, relight the center of three engines, and fly back to the launch site following a ballistic trajectory. Parachutes would be used to decelerate the first stage for a soft landing on four airbags. The second-stage orbital vehicle (OV) carries the payload to orbit, deorbits, and returns to Earth flying a mostly ballistic trajectory but with the OV's AoA oriented to create some lifting. Anticipated blackout for this stage is discussed in the next section.

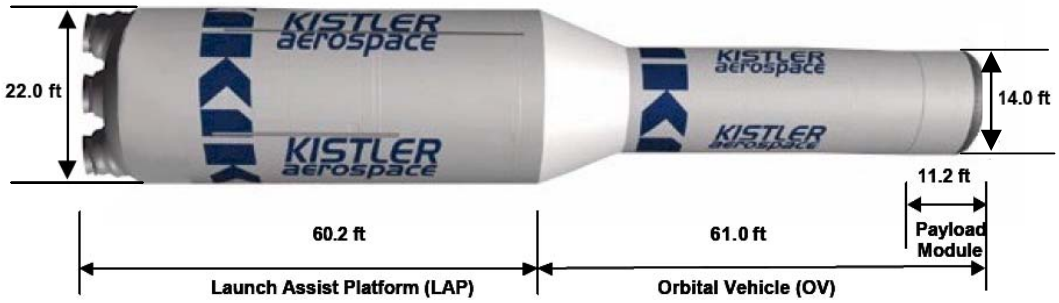

Figure 9. K-1 vehicle profile. *(Reprinted with permission of Rocketplane Kistler, Inc).*

V. Blackout Trajectories for Four Vehicle Classes

Blackout trajectories and times for reentry of the Shuttle, the RpK OV, the RAM C, and sharp-tipped RVs are compared in Fig. 10. The absence of blackout for very sharp RVs is of key importance. Of special interest is a comparison of the trajectory of the RpK OV to that of the Space Shuttle Orbiter, which reveals that the OV retains considerably higher velocity at each equivalent altitude. The significantly longer blackout time for the Shuttle (16 minutes) relative to that for the RpK OV (1 minute) results from the fact that the Shuttle is a lifting body that reenters the atmosphere at a 40º AoA to produce deceleration at high altitudes, thereby reducing heat transfer to the vehicle thermal protection system, while the K-1 essentially follows a fast ballistic trajectory, taking only one minute to descend from a very high altitude to a low altitude where recovery from blackout can occur. The Shuttle experiences blackout onset at 265 kft and recovers at 162 kft. We would expect the OV to have the same or higher onset altitude (both at 25 kft/s velocity) and to recover from blackout when it slows down to a velocity of 9 kft/s, which occurs at an altitude of 110 kft. Velocity is the major determinant of the maximum temperature in the flow field, and temperature is the major determinant of degree of ionization in the flow.

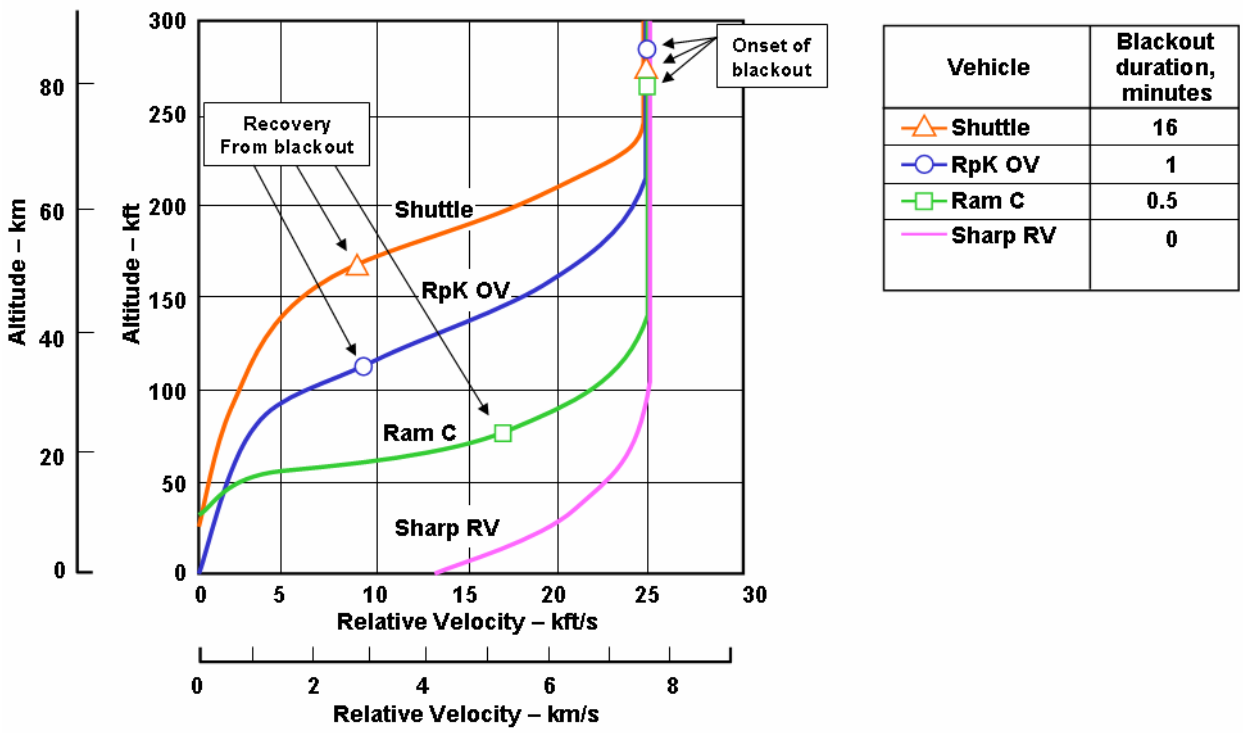

Figure 10. Blackout trajectories for four vehicle classes

VI. Blackout Mitigation Strategies

Five proposed techniques for mitigating blackout were identified, and recommendations were made regarding their relative promise for application to future commercial space transportation systems. The techniques that were evaluated were: aerodynamic shaping, injection of liquid electrophilic quenchants into the plasma sheath, application of a magnetic field, use of high frequencies, and use of high power. These approaches are discussed in the sections that follow.

A. Aerodynamic Shaping

A promising example of aerodynamic shaping is illustrated in Fig. 11. In this example, a sharp, slender probe containing an antenna projects ahead of the bow shock of a blunt-nose vehicle. Belov et al. have done considerable analysis and experimental evaluation of the aerodynamics, heat transfer, and nose radius required to assure sufficiently low electron density flowing aft, where the antenna is located.[8] The sharp nose-cone of the probe is a porous sintered metal, selected to accommodate cold gas cooling for survival.

B. Injection of Liquid Electrophilic Quenchants

NASA has conducted successful flight demonstrations of the injection of liquids into the flow to alleviate blackout. One demonstration was on the Gemini 3 Reentry capsule manned by two astronauts on March 23, 1965.[9] Significant levels of signal strength increase during the early portion of a water injection sequence over an altitude range of 272 to 246 kft were detected by VHF telemetry and VHF voice ground stations. Enhancement of C-band beacon signal was observed during the latter portion of the water injection sequence from 200- to 160-kft altitude. A comparison of calculated electron concentrations showed the same trends. This comparison was based on an assumption that the primary mechanism of electron concentration reduction is recombination at or near the surface of water drops, with values deduced from the observed VHF attenuation data. The data from this flight provided evidence that it is possible to alleviate RF attenuation on a blunt body by water injection in the flow field.

C. Application of Magnetic Field

Theory supports the concept of applying a magnetic field to alleviate blackout, and laboratory experiments at NASA-Langley concluded that a 750 Gauss magnetic field resulted in a 20 dB reduction in VHF attenuation, from 60 dB to 40 dB.

Starkey et al. analyzed a hypothetical air-breathing vehicle with very blunt leading edges (6-in. radius) and showed that this configuration generates thick plasma layers with very high electron density.[10] A calculated magnetic field strength of 10^4 Gauss was required to penetrate this substantial plasma layer. However, no reasonable air-breathing vehicle will have leading-edge radii that large.

Usui et al. concluded from an analytical experiment that use of the Whistler mode (where the magnetic field cyclotron frequency equals the RF frequency) could provide a window for RF transmission using a magnetic field strength of 1500 Gauss.[11]

Whereas current magnetic field strength generation technology may support up to 1500 Gauss at acceptable weight and volume, achieving 10^4 Gauss will require significant advances in superconducting technologies.

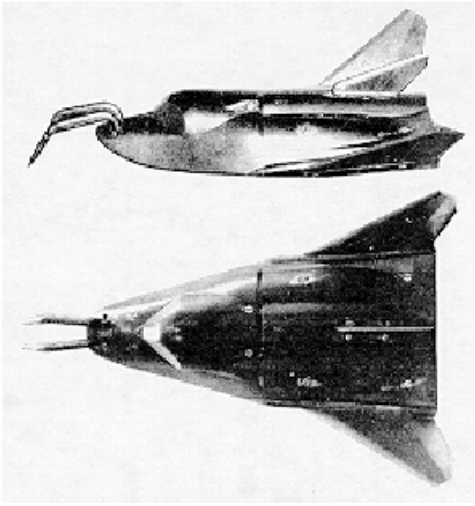

Figure 11. Sharp slender probe projecting ahead of blunt-nose vehicle shock bow wave.[8] *(Reprinted with permission of AIAA).*

D. Other Mitigation Approaches Considered

Two other RF blackout mitigation strategies were studied: use of high frequencies and use of high power. Although increasing the frequency generally reduces attenuation, higher frequencies are more subject to atmospheric and rain attenuation, with 10 GHz often suggested as a practical upper limit.

Transmitting higher power from the vehicle is limited by aperture breakdown, with typical breakdown powers in the range of hundreds of watts. Increasing the transmit power to compensate, as an example, for even 30 dB of attenuation is clearly impractical.

E. Summary of Blackout Mitigation Strategies

RF blackout mitigation strategies fall into two general classes: passive and active. Passive approaches necessitate attention to vehicle and antenna design to minimize plasma effects on communications signals. Active approaches entail manipulation of the plasma conditions and electron density in localized regions surrounding communication antennas to facilitate RF transmission.

Implementing one or a combination of passive approaches will minimize and possibly eliminate the blackout phenomenon. In our view, aerodynamic shaping, i.e., use of sharp leading edges, is the most practical and influential approach for mitigating blackout because generation of plasma causing blackout is minimized. However, there are limitations in implementing aerodynamic shaping and competing design requirements. For example, Belov et al. had to use cooling to protect a protruding sharp tip from the environment, making it an active system.[8]

Examples of active approaches to mitigating the RF blackout problem include: injection of chemical quenchants, or droplets that evaporatively cool the plasma, and application of magnetic fields. These methods can be used periodically or locally where passive approaches are inadequate. Of these, the use of quenchants is the more well-established, practical method. Magnetic field mitigation holds some promise but has not been demonstrated sufficiently, and the implementation requirements appear daunting for existing technologies. Both of these active

approaches (quenchants and magnetic fields) could be advanced with additional experimental work to validate model calculations, particularly following a proposal by Usui et al. that unique "Whistler" modes may facilitate RF communications in a narrow range of resonant transmission frequencies.[11] However, use of sharp leading edges, as described above, can decrease the need for any of these active approaches.

VII. Conclusions and Recommendations

Several key conclusions were drawn from this study: First, sharp-tipped RVs experience little or no blackout if the nose radius and the angle of attack are small. The resulting very thin plasma sheath also facilitates other supplementary mitigation approaches, e.g., use of quenchants or magnetic fields, should they be necessary. In contrast to sharp-tipped vehicles, blunted conical and lifting-glide vehicles do experience significant blackout.

Aerodynamic shaping is the most promising approach for mitigating blackout and warrants further investigation. Designers of one vehicle class, i.e., powered hypersonic air-breathing vehicles, have great incentive to sharpen leading edges to reduce aerodynamic drag, which has the complementary benefit of making continuous RF communication more achievable. For RLVs with blunt-tipped configurations, the application of sharp, slender probes or cones containing antennas protruding ahead of the shock wave should be evaluated.

Higher frequencies were found to correlate with decreased blackout. However, atmospheric attenuation becomes an issue at frequencies greater than approximately 10 GHz. A detailed evaluation of appropriate spectra for RLV communications would be beneficial.

A detailed report on this study, prepared at The Aerospace Corporation, is posted on the website of the FAA Office of Commercial Space Transportation.[12]

Acknowledgments

This study was sponsored by the FAA Office of Commercial Space Transportation. Ms. Ann R. DiMare at the Volpe National Transportation Systems Center, U.S. Department of Transportation, served as the Contracting Officer's Technical Representative.

References

[1]Fuhs, A. E., "Flight Instrumentation for Reentry Plasma Sheath," *AIAA/Northwestern University Fifth Biennial Gas Dynamics Symposium*, AIAA Paper No. 1963-379, Aug 14-16, 1963.

[2]Steiger, M., Glatt, L., Fernandez, F., Fedele, J., and Golden, K., "Reentry Communication: Theoretical Analysis and Flight Test Results," *AIAA 8th Aerospace Sciences Meeting*, AIAA Paper No. 70-220, Jan 19-21, 1970.

[3]Dunn, M. G., and Kang, S. W., "Theoretical and Experimental Studies of Reentry Plasmas," NASA CR-2232, Apr 1973.

[4]Rybak, J. P., and Churchill, R. J., "Progress in Reentry Communications," *IEEE Trans. on Antennas and Propagation*, Vol. AES-7, No. 5, Sept 1971, pp. 879-894.

[5]Schexnayder, C. J., Evans, J. S., and Huber, P. W., "Comparison of Theoretical and Experimental Electron Density for RAM C Flights," *Proceedings, The Entry Plasma Sheath and its Effects on Space Vehicle Electromagnetic Systems,* Vol. I, NASA SP-252, NASA Langley Research Center, Oct 13-15, 1970, pp. 277-303.

[6]Jones, Jr., W. L., and Cross, A. E., "Electrostatic Probe Measurements of Plasma Surrounding Three 25,000 Foot Per Second Reentry Flight Experiments," *Proceedings, The Entry Plasma Sheath and its Effects on Space Vehicle Electromagnetic Systems,* Vol. I, NASA SP-252, NASA Langley Research Center, Oct 13-15, 1970, pp. 109-136.

[7]Grantham, W. L., "Reentry Plasma Measurements Using a Four-Frequency Reflectometer," *Proceedings, The Entry Plasma Sheath and its Effects on Space Vehicle Electromagnetic Systems,* Vol. I, NASA SP-252, NASA Langley Research Center, Oct 13-15, 1970, pp. 65-107.

[8]Belov, I. F., Borovoy, V. Y., Gorelov, V. A., Kireev, A. Y., Korolev, A. S., and Stepanov, E. A., "Investigation of Remote Antenna Assembly for Radio Communication with Reentry Vehicle," *J. Spacecraft and Rockets* Vol. 38, No. 2, Mar-Apr 2001, pp. 249-256.

[9]Schroeder, L. C., and Russo, F. P., "Flight Investigation and Analysis of Alleviation of Communications Blackout by Water Injection During Gemini 3 Reentry," NASA TM X-1521, 1968.

[10]Starkey, R. P., "Electromagnetic Wave/Magnetoactive Plasma Sheath Interaction for Hypersonic Vehicle Telemetry Blackout Analysis," *34th AIAA Plasmadynamics and Lasers Conference*, 23-26 June 2003, p. 1.

[11]Usui, H., Matsumoto, H., Yamashita, F., Yamane, M., and Takenaka, S., "Computer Experiments on Radio Blackout of a Reentry Vehicle," *6th Spacecraft Charging Technology Conference*, AFRL-VS-TR-20001578, 1 Sept 2000, p. 107.

[12]Hartunian, R. A., Stewart, G. E., Fergason, S. D., Curtiss, T. J., and Seibold, R. W., "Causes and Mitigation of Radio Frequency (RF) Blackout During Reentry of Reusable Launch Vehicles," Final Report, U. S. Department of Transportation Contract DTRT57-05-D-30103, Task 7, Aerospace Corporation Report No. ATR-2007(5309)-1, Jan 26, 2007, URL: http://www.faa.gov/about/office_org/headquarters_offices/ast/reports_studies/media/ATR-2007(5309)-1.pdf [cited 02 July 2007].